Coverage-Mediated Suppression of Blinking in Solid State Quantum Dot Conjugated Organic Composite Nanostructures

Nathan I. Hammer,[†] Kevin T. Early,[†] Kevin Sill,[‡] Michael Y. Odoi,[†] Todd Emrick,[‡] and Michael D. Barnes*,[†]

The George Richason, Jr. Chemistry Research Laboratory, Department of Chemistry and Department of Polymer Science & Engineering, University of Massachusetts, Amherst, Massachusetts 01003

Received: April 3, 2006; In Final Form: May 20, 2006

Size-correlated single-molecule fluorescence measurements on CdSe quantum dots functionalized with oligo(phenylene vinylene) (OPV) ligands exhibit modified fluorescence intermittency (blinking) statistics that are highly sensitive to the degree of ligand coverage on the quantum dot surface. As evidenced by a distinct surface height signature, fully covered CdSe−OPV nanostructures (~25 ligands) show complete suppression of blinking in the solid state on an integration time scale of 1 s. Some access to dark states is observed on finer time scales (100 ms) with average persistence times significantly shorter than those from ZnS-capped CdSe quantum dots. This effect is interpreted as resulting from charge transport from photoexcited OPV into vacant trap sites on the quantum dot surface. These results suggest exciting new applications of composite quantum dot/organic systems in optoelectronic systems.

Introduction

Fluorescence intermittency, or "blinking", in quantum dot systems has been the subject of both great fundamental interest and frustration since the first observation of this phenomenon nearly 10 years ago.[1−3] While the statistical properties of quantum dot blinking have been studied as a function of structural and environmental parameters,[1−8] surprisingly little is known about specific ways to suppress it.[9,10] The stability of quantum dot fluorescence emission is especially important in the context of photovoltaic, optoelectronic, and biological applications, where device performance, or the ability to track labeled particles, is affected adversely by fluorescence intermittency.[11−18] Here, we demonstrate for the first time efficient suppression of quantum dot blinking in CdSe quantum dots whose surfaces are coordinated with varying numbers of conjugated organic ligands (oligo(phenylene vinylene), OPV). Size-correlated fluorescence measurements show that the degree of blinking suppression is highly sensitive to the ligand coverage on the quantum dot surface. This interesting new class of inorganic/organic nanocomposite material functions essentially as quantum dots but with significantly enhanced temporal and spectral stability. This represents a significant advance in modification of photophysical properties of quantum dot/organic composites and is an important step toward their successful incorporation into optoelectronic devices.

Emrick and co-workers recently demonstrated efficient synthesis of quantum dot−organic composite nanostructures with conjugated organic ligands coordinated directly to the quantum dot surface.[19] The direct surface derivatization with organic ligands enables a "tunable" quantum dot surface allowing dispersion of quantum dots in a variety of polymer-supported thin films[20,21] without phase segregation, which facilitates straightforward inclusion in solid-state formats. Recent single-molecule fluorescence studies in our laboratory show fluorescence spectra from individual CdSe−OPV nanostructures that are significantly modified with respect to bulk blended films of the same components.[22] The emission spectra from these species were observed to be dominated by the quantum dot, implying efficient energy transfer from the conjugated organic ligands. Figure 1 shows representative absorption and emission spectra of the components of CdSe−OPV along with the emission spectrum from a single CdSe−OPV nanostructure. The observation of efficient energy transfer was attributed to the molecular architecture that facilitated much closer (≈3×) center-to-center chromophore spacings than estimated in bulk blends.[23]

In addition to energy transfer between the quantum dot and the conjugated organic ligands, photophysical properties of the CdSe−OPV nanostructures were found to be enhanced. One important observation was the apparent suppression of blinking in emission from the quantum dots.[22] Shown in Figure 2 are time-resolved fluorescence spectra for two CdSe−OPV nanostructures, taken with exposure times of (a) 2 s and (b) 300 ms. The spectra in (a) reveal only a small amount of OPV emission (approximately 20−30% of the total integrated fluorescence), whereas those shown in (b) exhibit only quantum dot emission. This is seen clearly in (c) and (d) where fluorescence time traces for these nanostructures have been separated into the different spectral components (black, quantum dot; gray, OPV). For these exposure times we do not observe true quantum dot dark states; $\langle\tau_{off}\rangle \approx 0$, compared with $\langle\tau_{off}\rangle \approx 9$ s for CdSe/ZnS. Only for shorter exposure times did the dark state become apparent.

As illustrated in Figure 3, we observed minimal spectral diffusion in the CdSe−OPV nanostructures. Typical fluctuations in the peak emission wavelength for a CdSe−OPV nanostructure were contained within $\approx^1/_2$ the quantum dot (QD) fwhm; that is $[\langle\lambda^2\rangle - \langle\lambda\rangle^2]^{1/2} \approx 10$ nm. Whereas the peak wavelength from the DOPO−Br covered CdSe quantum dot quickly blue-shifts due to surface oxidation, the CdSe−OPV peak wavelength,

* To whom correspondence may be addressed. E-mail: mdbarnes@chem.umass.edu.
[†] Department of Chemistry
[‡] Department of Polymer Science & Engineering.

10.1021/jp062065f CCC: $33.50
Published on Web 06/27/2006

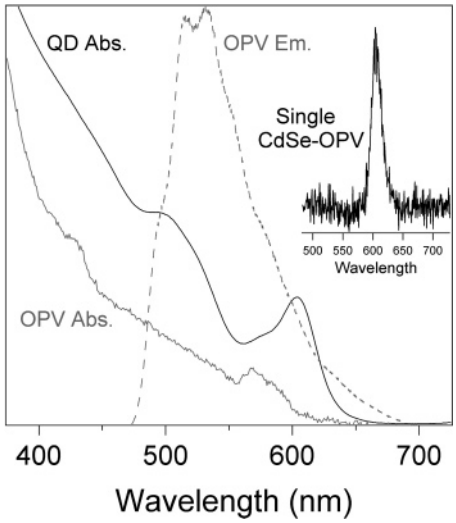

Figure 1. Absorption spectra of bulk solid-state OPV (gray) and CdSe quantum dots (~4.5 nm, black) and emission spectra from bulk OPV (dotted gray) and a single CdSe−OPV nanostructure (black, inset) excited at 457 nm.

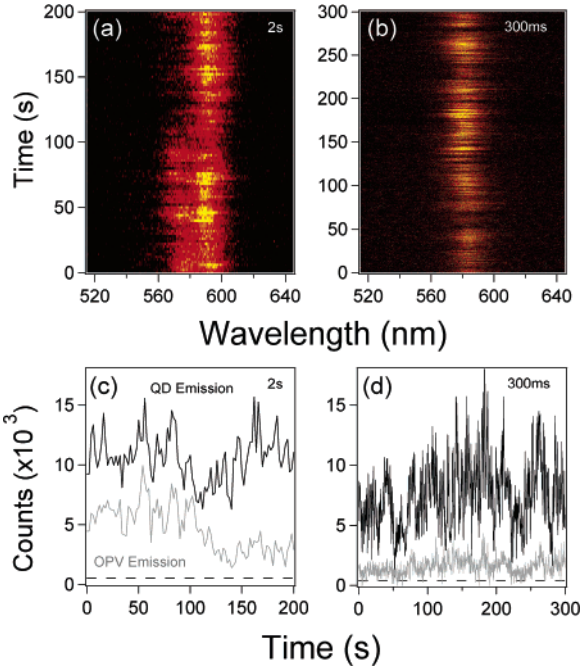

Figure 2. Time-resolved fluorescence spectra from two CdSe−OPV nanostructures: (a) 2 s exposure time and (b) 300 ms exposure time. The spectrally resolved emission profiles showing the quantum dot (black) and OPV (gray) components for (a) and (b) are shown in (c) and (d), respectively. The dotted lines in (c) and (d) represent $+2\sigma$ with respect to the mean background.

taken from the spectra in Figure 2a, remains consistent, similar to that observed from a ZnS-capped quantum dot of similar size.

One of the interesting features of this system is a significant heterogeneity in the photophysical response within a CdSe−OPV sample. This suggests that the fluorescence properties of an individual nanostructure might be linked to structural details not apparent by optical studies alone. Here, we show that the degree of fluorescence intermittency in CdSe−OPV nanostructures is correlated strongly with a ligand coverage dimension inferred from atomic force microscope (AFM) measurements. By integrating the fluorescence measurements with surface height signatures obtained by AFM, we obtain new insights into

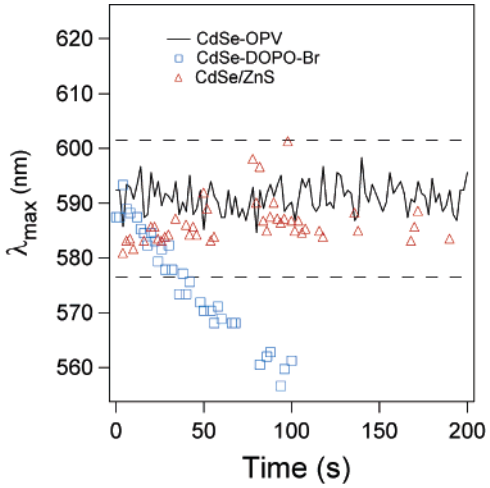

Figure 3. Spectral fluctuations of a CdSe−OPV nanostructure compared with that of representative DOPO−Br covered and ZnS-capped CdSe quantum dots. The dotted lines indicate the ±fwhm of the quantum dot emission peak and the exposure time was 2 s.

the coverage-dependent photophysics of this interesting composite nanosystem.

Experimental Section

The quantum dot−OPV composite nanomaterials used in this study were prepared by growing the OPV ligands from phenyl bromide functionalized ~4.3 nm diameter CdSe quantum dots, where OPV coordinates to the CdSe surface through chain-end phosphine oxides.[19,22] Matrix-assisted laser desorption/ionization time-of-flight (MALDI-TOF) mass spectrometry measurements were performed to determine the distribution of OPV ligand lengths. Individual CdSe−OPV nanostructures were isolated from dilute tetrahydrofuran solution (~10^{-10} M) on clean glass coverslips. We used 457-nm radiation from a continuous wave Ar^+ laser (≈ 200 μW power; 15 μm diameter spot size) as the excitation source. All fluorescence imaging and spectroscopic measurements were obtained under ambient conditions using a Nikon TE300 inverted microscope with a 1.4 NA oil objective in a total internal reflectance (TIR) configuration. AFM measurements were performed in Tapping Mode using a Digital Instruments Bioscope model BS3-N mounted directly to the microscope. Fluorescence images were acquired with a Princeton Instruments PhotonMax CCD camera, with exposure times of 100 ms to 2 s and a typical total observation time of 1000 s. Spectra were acquired by focusing the QD-OPV emission from the side-port of the microscope onto an Acton SP2150i dual-grating spectrograph and detected with a Roper Scientific Pixis 400B back-illuminated CCD. Initial registration of fluorescence and AFM surface height images was performed using 20-nm FluoSpheres (Invitrogen Corporation).[24]

Results and Discussion

Figure 4 shows a typical fluorescence image from a dilute sample of CdSe−OPV nanostructures and the corresponding AFM surface height image from the same region. The inset in (b) illustrates a representative height trace for a particular nanostructure indicated by the circle. Figure 4c shows the spectrally integrated fluorescence intensity as a function of time for this same nanostructure compared with that of a representative ZnS-capped 4.3 nm CdSe quantum dot (Figure 4d) with the $+2\sigma$ threshold (with respect to the mean background) indicated by the dashed lines. Typical fluorescence profiles from

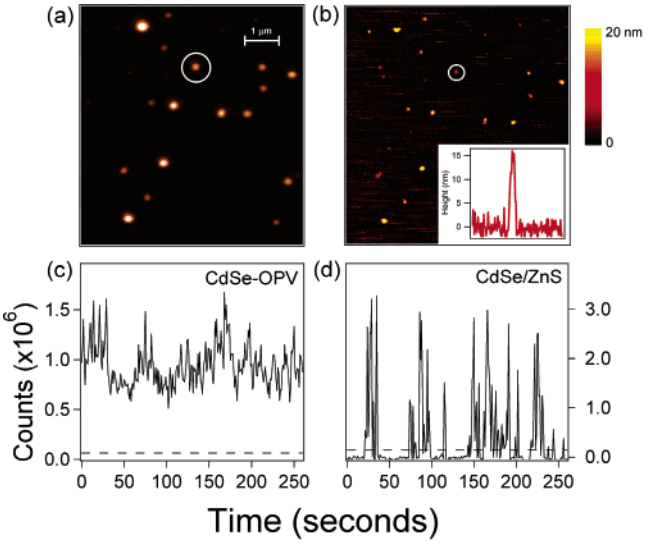

Figure 4. Correlation of single particle fluorescence with AFM height signatures: (a) fluorescence and (b) AFM images of the same CdSe−OPV nanostructures and (c) fluorescence time trace of the circled nanostructure compared to (d) fluorescence time trace of a representative ZnS-capped CdSe quantum dot. A height trace of the circled nanostructure is included in (b) and the dotted lines in (c) and (d) represent 2σ with respect to the mean background. The background was determined by examining the fluorescence intensity from pixels surrounding the CdSe−OPV emission.

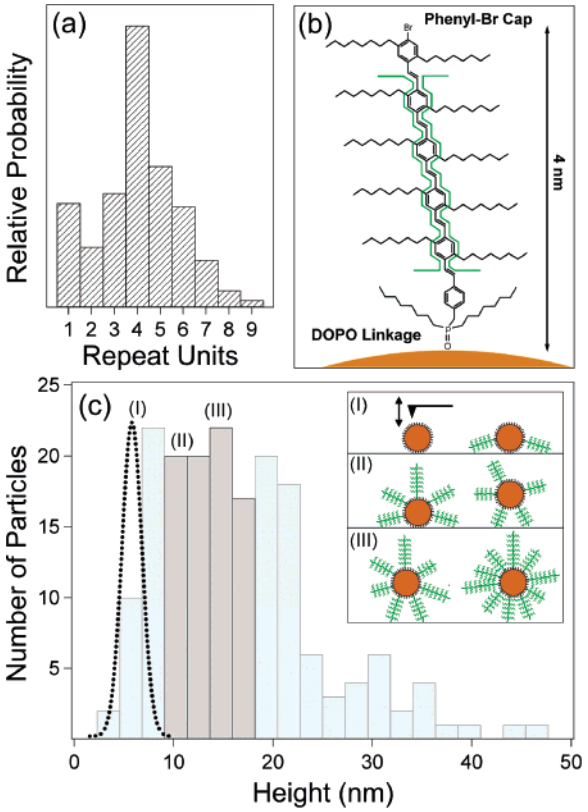

Figure 5. Physical characterization of CdSe−OPV: (a) distribution of OPV ligand lengths obtained from MALDI measurements, (b) structure and length of an OPV ligand with three monomer repeat units, and (c) measured size distributions of 180 CdSe−OPV nanoparticles (block histogram) and their synthetic precursors—phenyl bromide covered CdSe quantum dots (dotted curve). The inset in (c) shows a schematic of possible ligand arrangements corresponding to the various size regimes: I, sparse coverage; II, intermediate coverage; III, high coverage.

ZnS-capped CdSe quantum dots exhibit significant intensity fluctuations and dark periods lasting tens of seconds. In contrast, the fluorescence intensity for this particular CdSe−OPV nanostructure in Figure 4c is at all times well above the noise thresholds. The lack of blinking observed in the integrated fluorescence from CdSe−OPV nanostructures cannot be explained by supplemental emission from the OPV ligands, as the fluorescence spectra from individual CdSe−OPV nanostructures are dominated by the quantum dot.[22]

The AFM height signatures of single CdSe−OPV nanostructures, referenced to those of CdSe quantum dots without the additional conjugated organic ligands, allow us to infer a coverage dimension based on knowledge of the distribution of ligand length. MALDI-TOF measurements show an approximately Poissonian distribution of OPV chain lengths, with an average of four monomer repeat units (five OPV units plus a phenyl-Br cap and DOPO linkage). This distribution is shown in Figure 5a, along with the structure of an OPV ligand with three monomer repeat units in Figure 5b. The length of an OPV ligand with four monomer repeat units is approximately 4.5 nm. For essentially complete ligand coverage, the average surface height of a CdSe−OPV nanostructure should be determined to good approximation by the sum of the quantum dot diameter (4.3 nm) and twice the average ligand length to yield $d_{avg} \approx$ 13−14 nm. This should be an accurate estimation since the persistence length of polyphenylene vinylene derivatives (≈10 nm) has been shown to be greater than the ligand lengths studied here.[25] Surface pressure could, however, give rise to OPV ligands not perpendicular to the quantum dot surface and therefore lower height signatures, although the polymerization of OPV directly onto the quantum dot promotes an orientation normal to the surface.

Figure 5c shows a histogram of measured heights of 180 CdSe−OPV nanostructures, along with structural schematics depicting some of the possible ligand arrangements consistent with the measured surface heights. Also included in Figure 5c is an AFM size distribution of the CdSe quantum dot precursor (dotted line). We observe a small overlap between the CdSe−OPV and bare quantum dot size distributions, indicating that a small fraction (∼10%) of the composite nanostructures (labeled **I**) has sparse or nil OPV coverage or ligands that are nonnormal to the quantum dot surface. Slightly larger height signatures (labeled **II**) would therefore indicate nanostructures that have an intermediate degree of OPV ligand coverage. A number of different arrangements are possible in this size regime that yield surface heights less than the maximum possible value. Those nanostructures that we interpret as exhibiting essentially complete coverage (labeled **III**), demonstrate a distribution of height signatures that mimics that of the OPV ligand length. We believe height signatures greater than ∼20 nm—representing a small percent of the total CdSe−OPV sample—are likely associated with nanostructure aggregates and therefore omit them from consideration.

To quantify the fluorescence intermittency of individual nanoparticles, we define the fluorescence "duty factor" (FDF) as the fraction of time the fluorescence is measured in an "*on*" state relative to the total time of the observation. The distinction between "*on*" and "*off* " is made by a 2σ threshold test of a particular fluorescence intensity measurement relative to the mean background level, determined by examining the pixels surrounding the diffraction-limited CdSe−OPV nanoparticle fluorescence image. This characterization is related to the common power-law kinetics, $P(\tau_{off}) = 1/\tau_{off}^{\alpha+1}$, description,[3] which has been employed previously to describe quantum dot blinking. Here, however, a larger number of the quantum dots

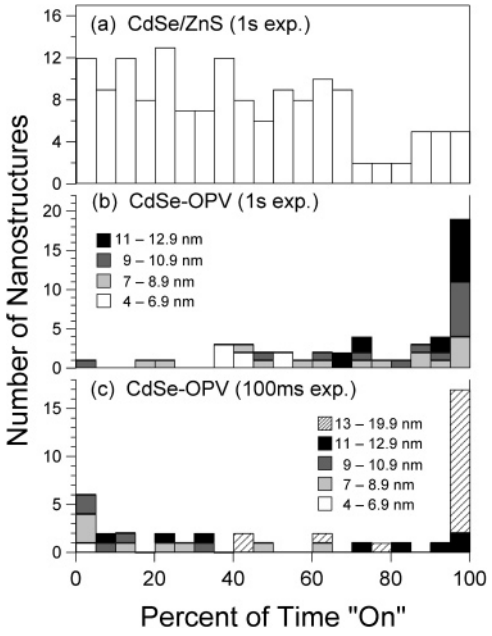

Figure 6. Histogram of fluorescence duty factors from (a) 4.3 nm ZnS-capped CdSe quantum dots; (b) and (c) CdSe−OPV nanostructures sorted using size-correlated measurements into the following classes: 4−6.9, 7−8.9, 9−10.9, 11−12.9, and 13−19.9 nm. The exposure time in (a) and (b) was 1 s and in (c) 100 ms. Fluorescence duty factors are defined by the percentage of time fluorescence emission is greater than the 2σ threshold referenced to the mean background.

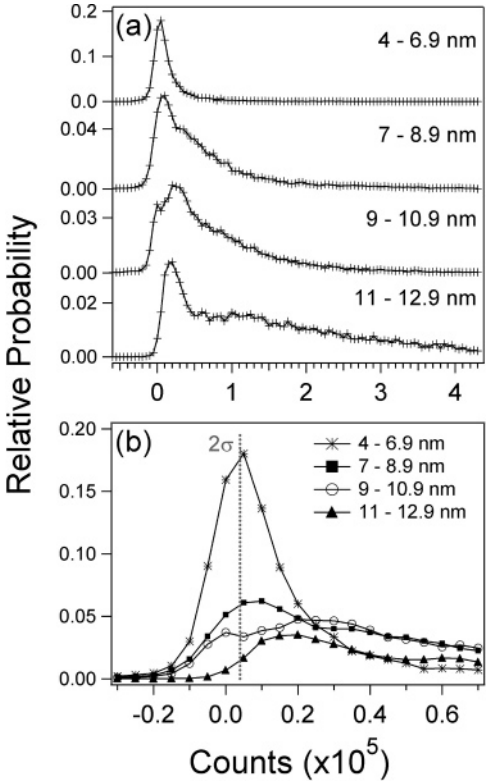

Figure 7. Histograms showing the relative probability of emission intensity from individual CdSe−OPV nanostructures for different size classes taken from Figure 6b. A magnification of (a) near the 2σ threshold (dotted line) is shown in (b). Integrated intensities greater than the 2σ threshold represent the average duty factors for those size classes.

never blink and therefore a more appropriate description of the blinking statistics is the average off time $\langle\tau_{off}\rangle$.

Figure 6 shows a histogram of the fluorescence duty factor for CdSe−OPV nanostructures with measured particle sizes at two different exposure times compared with those from ZnS-capped CdSe quantum dots. With an exposure time of 1 s, the conventional ZnS-capped quantum dots exhibit FDFs ranging from 1% to 95% with a mean of ≈40% (Figure 6a). This behavior differs significantly from that observed from our sample of CdSe−OPV nanostructures, shown by gray scale coding of particle size in the fluorescence duty-factor histogram (Figure 6b). Only data from CdSe−OPV nanoparticles with a measured height less than 13 nm were included in Figure 6b to avoid possible contributions from clusters of nanostructures. For CdSe−OPV nanostructures in the size range of 4−7 nm, the blinking statistics were indistinguishable from "bare" quantum dots. In the size range of 7−10 nm, the average fluorescence duty factor is ≈70%, while particles in the size range of 11−13 nm (nanostructures with a high degree of ligand coverage) show a fluorescence duty factor approaching 100%. These data show clearly the correlation between particle size (related to ligand concentration on the quantum dot surface) and blinking statistics. At the shorter exposure time (100 ms), summarized in Figure 6c, the correlation of blinking suppression with coverage is maintained. However, these data show that blinking is only apparent at much shorter exposure times than with underivatized quantum dots. At this exposure time (100 ms), $\langle\tau_{off}\rangle \approx 500$ ms for nanostructures in the 11−12.9 size range.

While we do not see oscillation between "on" and "off" states (at an exposure time of 1 s) in the nanostructures exhibiting a higher ligand coverage like in ZnS-capped CdSe quantum dots, we do observe significant fluctuations. Shown in Figure 7 are cumulative histograms showing relative probability of intensities for the four size classes studied in Figure 6b. Quantum dots with little or no OPV coverage (4−6.9 nm) display intensities peaked around the average 2σ reference with an average intensity of 2.1×10^4 counts. Quantum dots with increasing OPV coverages (7−8.9 nm and 9−10.9 nm size classes) exhibit markedly higher average intensity values (7.3×10^4 and 8.2×10^4 counts, respectively). CdSe nanostructures in the size range consistent with high OPV coverage (11−12.9 nm) exhibit an average intensity of 1.7×10^5 counts. The integrated intensities greater than the 2σ reference level shown in Figure 7b represent the average duty factors for those size classes. Whereas the intensity profile for the sparsely covered quantum dots appears simple and for the most part symmetric, those for the quantum dots with higher coverages appear more complicated. This suggests that there is a dynamic process at play in the blinking suppression mechanism.

We propose that the mechanism for suppressed blinking in CdSe−OPV nanostructures involves charge transfer from excited OPV ligands to vacant surface trap sites on the quantum dot. On the basis of estimates of relative electron affinities, transport of photoproduced charge carriers in the OPV ligands to the quantum dot is energetically favored where they fill surface trap sites.[20] This, in turn, enhances the radiative recombination probability within the quantum dot by restricting the number of available trap sites to excitons created within the quantum dot. This conclusion is consistent with our size-correlated results where a higher OPV surface concentration is associated with larger fluorescence duty factor as a result of fewer available trap sites. Ha and co-workers observed similar effects in solution where the choice of thiol-containing ligands for surface passivation reduced blinking.[9] In that work the authors postulated that β-mercaptoethanol molecules served as electron donating moieties to the quantum dot surface—thus inhibiting blinking via diminished vacancy for surface trap sites. Our work is consistent with a similar mechanism whereby

charge transport from the OPV to the quantum dot is facilitated by optical excitation. More recently, Tinnefeld and co-workers[10] demonstrated that quantum dots in contact with mercaptoethylamine exhibited reduced blinking but also increased blinking kinetics on a time scale less than 10 ms. Such an increase in blinking kinetics here would similarly result in the observed decrease in $\langle\tau_{off}\rangle$.

Conclusions

We have shown that fluorescence blinking in quantum dot systems coordinated with conjugated OPV organic ligands can be significantly modified for particles with a high coverage of the ligand. Combined single molecule fluorescence and scanning probe microscopy studies on individual CdSe−OPV composite nanostructures reveal a clear connection between blinking suppression and the degree of ligand coverage. For nanostructures in the size range of 11−13 nm (a surface height in agreement with a quantum dot fully coordinated with 3−4 nm OPV ligands), we observe an average fluorescence duty factor of greater than 90% using an exposure time of 1 s. In contrast, nanostructures in the size range of 4−7 nm, suggesting a low coverage of the ligands, show fluorescence duty factors similar to conventional alkane-covered quantum dots (<50%). This behavior is expected to track with the size of the quantum dot and should allow for the tailored synthesis of nanostructures with tunable properties. These new materials could be used in nanoscale optoelectronic contexts, such as high-sensitivity sensor and focal plane array applications, and could serve as new efficient nanoscale single-photon sources for use in quantum informatics.

Acknowledgment. We wish to thank the Intelligence Community Postdoctoral Research Fellowship Program and the U.S. Department of Energy Office of Basic Energy Sciences (Grant #05ER15695) for support of this work.

References and Notes

(1) Nirmal, M.; Dabbousi, B. O.; Bawendi, M. G.; Macklin, J. J.; Trautman, J. K.; Harris, T. D.; Brus, L. E. *Nature* **1996**, *383*, 802.

(2) Efros, A. L.; Rosen, M. *Phys. Rev. Lett.* **1997**, *78*, 1110.

(3) Kuno, M.; Fromm, D. P.; Hamann, H. F.; Gallagher, A.; Nesbitt, D. J. *J. Chem. Phys.* **2000**, *112*, 3117.

(4) Neuhauser, R. G.; Shimizu, K. T.; Woo, W. K.; Empedocles, S. A.; Bawendi, M. G. *Phys. Rev. Lett.* **2000**, *85*, 3301.

(5) Shimizu, K. T.; Woo, W. K.; Fisher, B. R.; Eisler, H. J.; Bawendi, M. G. *Phys. Rev. Lett.* **2002**, *89*, 117401

(6) Chung, I. H.; Bawendi, M. G. *Phys. Rev. B* **2004**, *70*, 165304

(7) Pelton, M.; Grier, D. G.; Guyot-Sionnest, P. *Appl. Phys. Lett.* **2004**, *85*, 819.

(8) Frantsuzov, P. A.; Marcus, R. A. *Phys. Rev. B* **2005**, *72*, 155321

(9) Hohng, S.; Ha, T. *J. Am. Chem. Soc.* **2004**, *126*, 1324.

(10) Biebricher, A.; Sauer, M.; Tinnefeld, P. *J. Phys. Chem. B* **2006**, *110*, 5174.

(11) Colvin, V. L.; Schlamp, M. C.; Alivisatos, A. P. *Nature* **1994**, *370*, 354.

(12) Mattoussi, H.; Radzilowski, L. H.; Dabbousi, B. O.; Thomas, E. L.; Bawendi, M. G.; Rubner, M. F. *J. Appl. Phys.* **1998**, *83*, 7965.

(13) Lee, J.; Sundar, V. C.; Heine, J. R.; Bawendi, M. G.; Jensen, K. F. *Adv. Mater.* **2000**, *12*, 1102.

(14) Coe, S.; Woo, W. K.; Bawendi, M.; Bulovic, V. *Nature* **2002**, *420*, 800.

(15) Tessler, N.; Medvedev, V.; Kazes, M.; Kan, S. H.; Banin, U. *Science* **2002**, *295*, 1506.

(16) Woo, W. K.; Shimizu, K. T.; Jarosz, M. V.; Neuhauser, R. G.; Leatherdale, C. A.; Rubner, M. A.; Bawendi, M. G. *Adv. Mater.* **2002**, *14*, 1068.

(17) Gur, I.; Fromer, N. A.; Geier, M. L.; Alivisatos, A. P. *Science* **2005**, *310*, 462.

(18) Zhang, C. Y.; Yeh, H. C.; Kuroki, M. T.; Wang, T. H. *Nat. Mater.* **2005**, *4*, 826.

(19) Skaff, H.; Sill, K.; Emrick, T. *J. Am. Chem. Soc.* **2004**, *126*, 11322.

(20) Greenham, N. C.; Peng, X. G.; Alivisatos, A. P. *Phys. Rev. B* **1996**, *54*, 17628.

(21) Mattoussi, H.; Radzilowski, L. H.; Dabbousi, B. O.; Fogg, D. E.; Schrock, R. R.; Thomas, E. L.; Rubner, M. F.; Bawendi, M. G. *J. Appl. Phys.* **1999**, *86*, 4390.

(22) Odoi, M. Y.; Hammer, N. I.; Sill, K.; Emrick, T.; Barnes, M. D. *J. Am. Chem. Soc.* **2006**, *128*, 3506.

(23) Anni, M.; Manna, L.; Cingolani, R.; Valerini, D.; Creti, A.; Lomascolo, M. *Appl. Phys. Lett.* **2004**, *85*, 4169.

(24) Mehta, A.; Thundat, T.; Barnes, M. D.; Chhabra, V.; Bhargava, R.; Bartko, A. P.; Dickson, R. M. *Appl. Opt.* **2003**, *42*, 2132.

(25) Gettinger, C. L.; Heeger, A. J.; Drake, J. M.; Pine, D. J. *J. Chem. Phys.* **1994**, *101*, 1673.